PHYSICAL REVIEW A **84**, 041807(R) (2011)

Realization of discrete quantum billiards in a two-dimensional optical lattice

Dmitry O. Krimer[1,2,*] and Ramaz Khomeriki[2,3,†]

[1]*Theoretische Physik, Universität Tübingen, Auf der Morgenstelle 14, D-72076 Tübingen, Germany*

[2]*Max-Planck Institute for the Physics of Complex Systems, Nöthnitzer Strasse 38, D-01187 Dresden, Germany*

[3]*Physics Department, Tbilisi State University, Chavchavadze 3, 0128 Tbilisi, Georgia*

(Received 23 May 2011; published 31 October 2011)

We propose a method for optical visualization of the Bose-Hubbard model with two interacting bosons in the form of two-dimensional (2D) optical lattices consisting of optical waveguides, where the waveguides at the diagonal are characterized by different refractive indices than others elsewhere, modeling the boson-boson interaction. We study the light intensity distribution function averaged over the direction of propagation for both ordered and disordered cases, exploring the sensitivity of the averaged picture with respect to the beam injection position. For our finite systems, the resulting patterns are reminiscent the ones set in billiards, and therefore we introduce a definition of discrete quantum billiards and discuss the possible relevance to its well-established continuous counterpart.

DOI: 10.1103/PhysRevA.84.041807 PACS number(s): 42.65.Wi, 67.85.−d, 03.65.Ge, 37.10.Jk

A very rich variety of wave phenomena originally discovered in the context of atomic and solid-state physics recently attracted much attention due to their analogy with optical systems. A prominent example is the Anderson localization, the phenomenon originally discovered as the localization of electronic wave function in disordered crystals [1] and later understood as a fundamental universal phenomenon of wave physics. Related recent experiments were performed on light propagation in spatially random nonlinear optical media [2,3] and on Bose-Einstein condensate expansions in random optical potentials [4]. A second example is the well-known solid-state problem of an electron in a periodic potential with an additional electric field, which led to investigations of Bloch oscillations and Landau-Zener tunneling in various physical systems such as ultracold atoms in optical lattices [5–7] and optical waves in photonic lattices [8,9]. Recent progress in the experiments stimulated a new turn in theoretical studies dealing with the evolution of a wave packet in nonlinear disordered chains [10] and in a nonlinear Stark ladder [11], and the effect of Anderson localization of light near boundaries of disordered photonic lattices [12], for example. Other examples are the classical analog of beam dynamics in one-dimensional (1D) photonic lattices to quantum coherent and displaced Fock states [13] and a classical realization of the two-site Bose-Hubbard model (applicable to the physics of strongly interacting many-body systems), based on light transport in engineered optical waveguide lattices [14].

In this Rapid Communication, we study a classical analog of a beam propagating in two-dimensional (2D) photonic lattice to quantum coherent dynamics of two particles in a 1D chain using the Bose-Hubbard model. We consider different situations ranging from the simple ordered case without interaction to the disordered case with interaction in our finite systems. Sometimes the resulting patterns pretty similar to the ones for the classical and/or quantum billiards, which are known to exhibit regular and chaotic behaviors (see, e.g., Ref. [15]). The advantage of our setup in comparison with traditional microwave realization of quantum billiards (where the measuring devices introduce additional perturbations in the system) is that the resulting quantum patterns could be simply observed as an optical image. We also emphasize the growing interest to the two-particle problem in the context of quantum correlations between two noninteracting particles evolving simultaneously in a disordered medium [16,17] and quantum walks of correlated photons, which provide a route to universal quantum computation [18]. Thus, the obtained

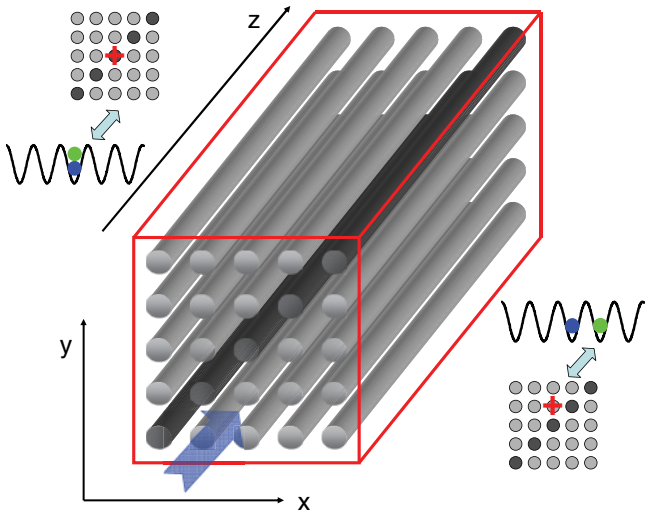

FIG. 1. (Color online) Geometry of setup: A beam enters the 2D optical lattice and propagates along the z axis. The refractivity index is constant along the z axis and is either periodic or disordered in transverse directions. The corresponding mapping to the dynamics of two interacting distinguishable bosons in a chain is also done (see the text for details). The interaction between bosons is introduced by taking the different from the rest refractive index for the diagonal waveguides. The injection of a beam to the diagonal waveguide mimics launching initially both bosons at the same site (upper inset), while injecting the beam into an off-diagonal waveguide corresponds to the two bosons located initially on different sites (lower inset).

*dmitry.krimer@gmail.com
†khomeriki@hotmail.com

 ©2011 American Physical Society

results might be applicable to both classical and quantum systems.

Let us introduce a standard Bose-Hubbard Hamiltonian describing two distinguishable bosons (or two fermions with opposite spins) in a chain with N sites:

$$\hat{\mathcal{H}} = \sum_{j=1}^{N} [(\hat{a}_{j+1}^{\dagger}\hat{a}_j + \hat{b}_{j+1}^{\dagger}\hat{b}_j + \text{H.c.}) + U\hat{a}_j^{\dagger}\hat{a}_j\hat{b}_j^{\dagger}\hat{b}_j], \quad (1)$$

where $\hat{b}_j^{\dagger}$ ($\hat{a}_j^{\dagger}$) and $\hat{b}_j$ ($\hat{a}_j$) are boson creation and annihilation operators on a lattice site j and U is the onsite interaction strength. Starting from the time-dependent Schrödinger equation $i\partial_t|\Psi(t)\rangle = \hat{\mathcal{H}}|\Psi(t)\rangle$, we expand $|\Psi(t)\rangle$ in terms of the N^2 orthonormal eigenstates of a number operator, $|m,n\rangle \equiv \hat{b}_m^{\dagger}\hat{a}_n^{\dagger}|0\rangle$, as $|\Psi(t)\rangle = \sum_{m,n=1}^{N} c_{mn}(t)|m,n\rangle$, where the amplitudes $c_{mn}(t)$ satisfy the following set of equations:

$$i\dot{c}_{mn} = U\delta_{mn}c_{mn} + \sum_{m',n'=1}^{N} R_{mn}^{m'n'}c_{m'n'}, \quad (2)$$

$$R_{mn}^{m'n'} = \delta_{m'm+1}\delta_{n'n} + \delta_{m',m-1}\delta_{n'n} + \delta_{m'm}\delta_{n'n+1} + \delta_{m'm}\delta_{n'n+1}.$$

Note that Eqs. (2) are invariant under permutation of m and n, and therefore it is natural to represent c_{mn} as a sum of symmetric $c_{mn}^{S} = (c_{mn} + c_{nm})/\sqrt{2}$ and antisymmetric $c_{mn}^{A} = (c_{mn} - c_{nm})/\sqrt{2}$ functions. In such a basis, the matrix $R_{mn}^{m'n'}$ is decomposed into two irreducible parts, one of which corresponds to the Bose-Hubbard model with two indistinguishable bosons and the other of which describes the physics of two indistinguishable spinless fermions. For the symmetric initial conditions, $c_{mn}(0) = c_{nm}(0)$, the dynamics is reduced to the former case (two indistinguishable bosons on sites m and n), whereas the latter case is realized for the antisymmetric initial conditions, $c_{mn}(0) = -c_{nm}(0)$.

Remarkably, Eqs. (2) are the same as the one used for the description of light propagation through 2D optical lattices [2] (for schematics, see Fig. 1) within the tight-binding approximation, where longitudinal dimension z plays a role of time. This approximation is valid when a lattice is constructed such that tunneling into nearest neighboring waveguides is allowed and there is a difference between the refractive indices of the diagonal n_d and off-diagonal n_0 waveguides which models the interaction (with the interaction strength $U \sim n_0 - n_d$). Thus, injecting a light beam at the waveguide with a position $x = m$, $y = n$ (asymmetric initial conditions) corresponds to the dynamics of two distinguishable interacting bosons in a chain, placed initially on sites m and n. One can also think about the Bose-Einstein condensate embedded into a 2D optical lattice, and then Eqs. (2) describe the evolution of some initial matter wave packet through the lattice.

In this Rapid Communication, we consider the system with hard boundaries having $c_{mn} = 0$ outside a square and monitor the time-averaged wave function

$$P_{mn} \equiv \lim_{T\to\infty} \frac{1}{T}\int_0^T |c_{mn}(t)|^2 dt, \quad (3)$$

referring to P_{mn} as to the averaged two-particle probability distribution function (PDF). To calculate PDFs we first solve the eigenvalue problem $\hat{\mathcal{H}}|q\rangle = \lambda_q|q\rangle$ and then expand $c_{mn}(t)$ with respect to the eigenvectors as

$$c_{mn}(t) = \sum_{q=1}^{N^2} \phi_q \mathcal{L}_{mn}^{(q)} e^{-i\lambda_q t}, \quad (4)$$

where $\mathcal{L}_{mn}^{(q)} \equiv \langle q|m,n\rangle$ is the eigenvector which belongs to the eigenvalue λ_q and $\phi_q \equiv \sum_{m,n=1}^{N} c_{mn}(0)\mathcal{L}_{mn}^{(q)}$ is its initial amplitude. Next, the averaged PDF is calculated by the following formula:

$$P_{mn} = \sum_{q} |\varphi_q|^2 \mathcal{L}_{mn}^{(q)2} + \sum_{i} \left| \sum_{q_i^r} \varphi_{q_i^r} \mathcal{L}_{mn}^{(q_i^r)} \right|^2, \quad (5)$$

where the first sum runs over all nondegenerate eigenvalues and the second sum corresponds to the summation with respect to r-fold degenerate eigenvalues λ_{q_i}.

Intuitively it seems that the light injected into one of the waveguides should spread over a whole lattice; however, the real situation is the opposite due to the interference from the hard boundaries. Let us start from the simplest noninteracting case, $U = 0$ (for the optical counterpart shown in Fig. 1, waveguides must all be identical). As seen from Fig. 2, a well-defined pattern for P_{mn} corresponds to each initial injection point. Thus, the system keeps the information about its initial state, and from the averaged picture one can recover an initial signal. It should be noted that these patterns might be strongly modified when the interaction is switched on, $U \neq 0$ (see Fig. 3). Remarkably, the pattern's structure is reminiscent of billiards, and therefore we introduce the notion of discrete quantum billiards and seek the analogies

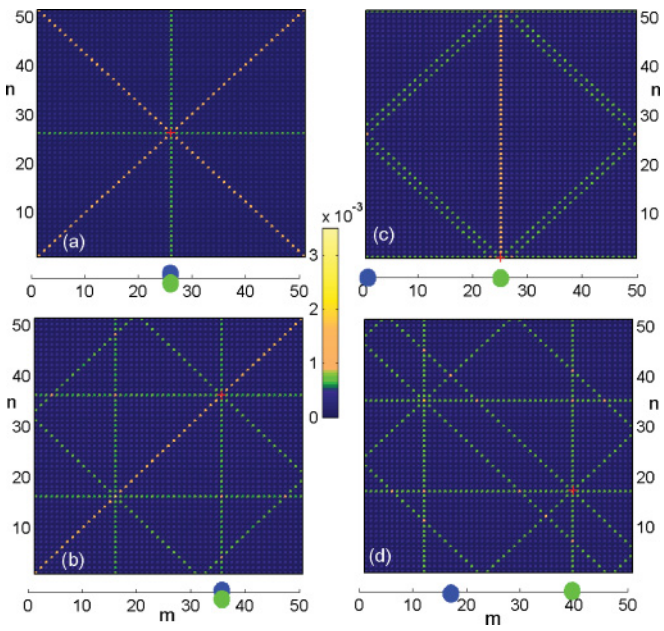

FIG. 2. (Color online) Characteristic pictures for discrete quantum billiard realization for different injection points depicted by a red cross in the absence of disorder and interaction ($W = 0$ and $U = 0$). In the main graphs, the averaged PDFs [see Eq. (3)] are displayed. The lower insets show the numbers of initially injected waveguides (or numbers of sites at which the particles are initially located).

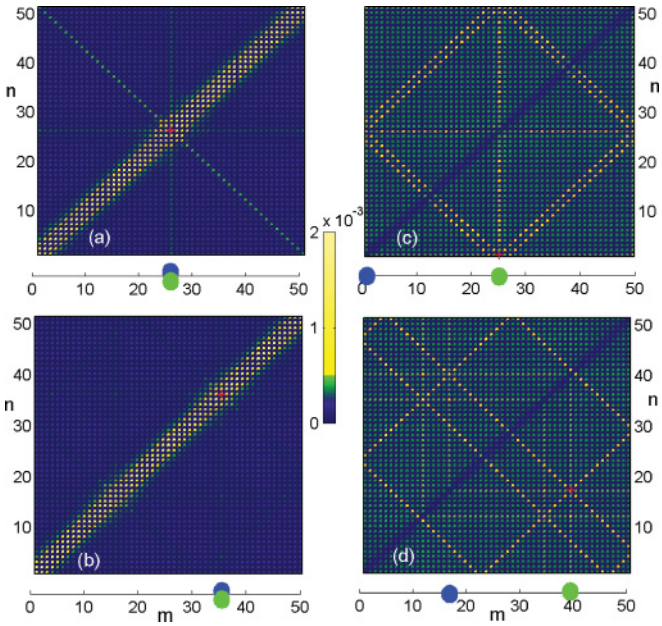

FIG. 3. (Color online) All parameters and quantities are the same as in Fig. 2, except the interaction constant $U = 1$.

with the usual continuous counterparts. The first step toward this direction is to explore the possibility of quantum chaos realization in such systems. We consider two possibilities to observe the transition toward quantum chaos. The first one is symmetry breaking by placing a square with rigid boundaries inside the system, as shown in Fig. 4. (Such a case has no analogy with the two-interacting-particles problem but might be realized using the optical lattices with a missing square area.) We monitor then the statistical properties of the eigenvalue spacings $s = |\lambda_{q+1} - \lambda_q|$ for different locations of the square, keeping injection point and interaction constant the same. It is seen that in the symmetric case the Poisson distribution

$$P(s) = 1/d e^{-s/d} \tag{6}$$

is realized, while for the asymmetric case the Wigner-Dyson distribution is observed:

$$P(s) = \pi s/(2d^2)\, e^{-\pi s^2/(4d^2)}. \tag{7}$$

Thus, the onset of quantum chaos can be visualized via the classical optical system of coupled waveguides.

The second mechanism of quantum chaos realization is an introduction of the disorder via adding the following terms to the Bose-Hubbard Hamiltonian (1):

$$\hat{\mathcal{H}}_d = \sum_{j=1}^{N} [\epsilon_j^a \hat{a}_j^\dagger \hat{a}_j + \epsilon_j^b \hat{b}_j^\dagger \hat{b}_j]. \tag{8}$$

Here ϵ_j^a and ϵ_j^b are two disorder potentials with random numbers from the interval $[-W/2, W/2]$, where W stands for the disorder strength. Finally, the modified evolution equations are

$$i\dot{c}_{mn} = (\mathcal{W}_{mn} + U\delta_{mn})\, c_{mn} + \sum_{m',n'=1}^{N} R_{mn}^{m'n'} c_{m'n'}, \tag{9}$$

where the matrix $R_{mn}^{m'n'}$ is given by Eq. (2) and $\mathcal{W}_{mn} = \epsilon_m^a + \epsilon_n^b$ are correlated disorder parameters. For the sake of simplicity, we take symmetric disorder $\epsilon_j^a = \epsilon_j^b$ that, together with symmetric initial conditions, corresponds to the dynamics of two interacting indistinguishable bosons or the beam

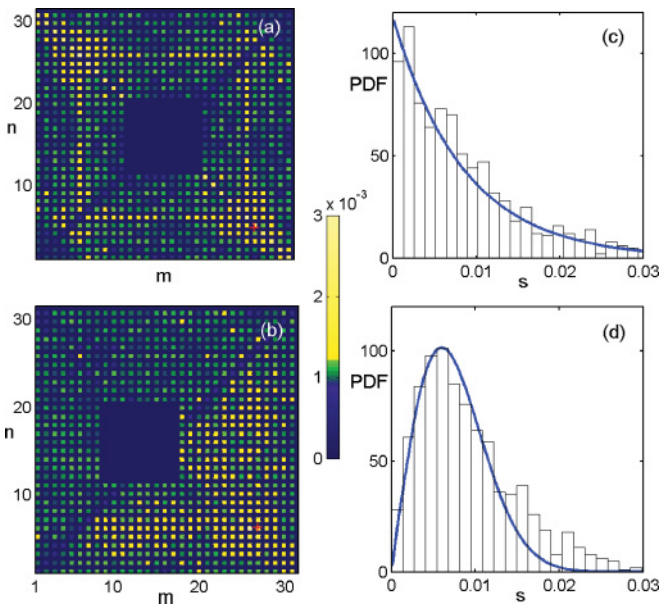

FIG. 4. (Color online) Characteristic pictures for discrete quantum billiard realization with a rigid square placed inside a system for the interaction constant $U = 1$ and the same injection point depicted by a red cross. (a), (b) Symmetric and asymmetric situations, respectively, with the corresponding probability density functions of eigenvalue spacings s shown in (c) and (d). (c) The Poisson distribution (6), with the average spacing $d = 0.0085$. (d) The Wigner-Dyson distribution (7), with the average spacing $d = 0.0075$.

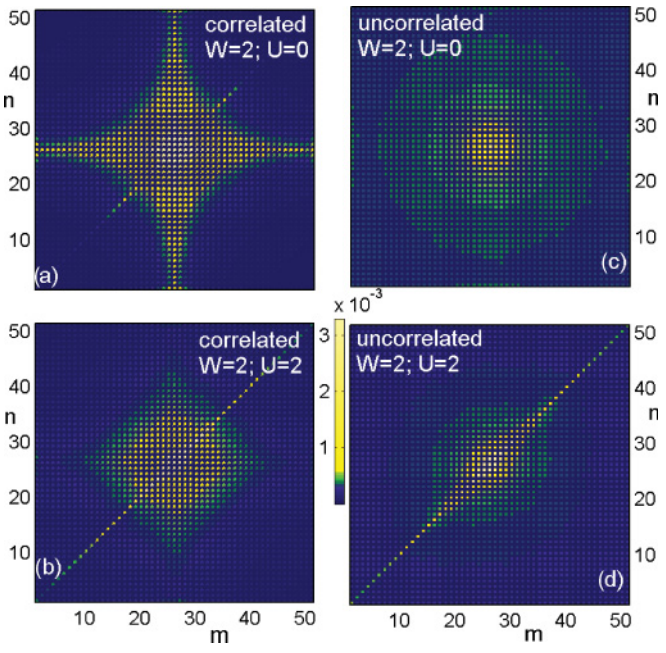

FIG. 5. (Color online) Averaged PDFs both in time and over many disorder realizations (all parameters are shown on the figures). The injection point in all graphs is taken at the middle of 2D optical lattice, $m = n = N/2$.

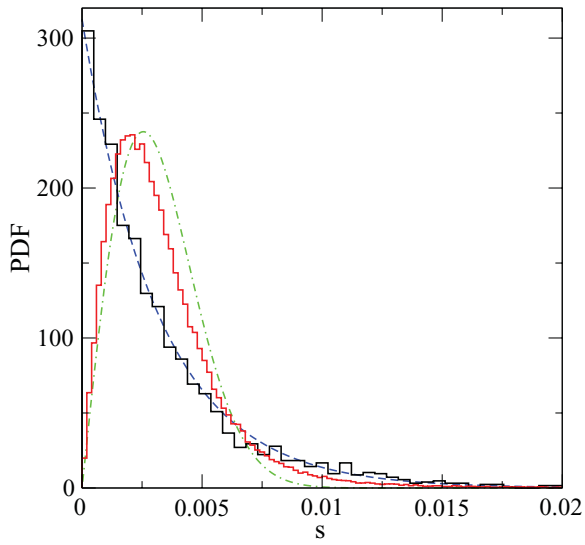

FIG. 6. (Color online) PDFs of eigenvalue spacings s for three different cases and a chain with $N = 51$ (the events with $s = 0$ due to degeneracy are not counted). Black curve: $W = 0$, $U = 2$ (disorder strength is zero only). Red curve (dark gray): $W = 2, U = 2$. The case with uncorrelated disorder is considered. Green dash-dotted curve: the Wigner-Dyson distribution (7), with the average spacing $d = 0.0032$. Blue dashed curve: the Poisson distribution (6), with the average spacing $d = 0.0032$.

propagation in 2D optical lattices. The typical structures for P_{mn}, averaged out with respect to many disorder realizations, are shown in Figs. 5(a) and 5(b). As is seen, the averaged PDFs demonstrate well-pronounced patterns, which look different than the case with a single disorder realization, when the PDF has many spots at different locations. For the noninteracting case, the PDF has an anisotropic structure with two distinct directions, $m = N/2$ and $n = N/2$, along which the particle motion mostly develops in average. Besides that, a slight contribution of two particle states is also visible. For $U = 2$, the interaction is already strong enough such that the contribution of states corresponding to the breather band becomes essential and the two particles mostly prefer to form a composite state and travel together.

Next, we consider the case of uncorrelated disorder [see Figs. 5(c) and 5(d)], taking $\mathcal{W}_{mn}$ as a sum of two independent random numbers for each m and n (thus generating $2N^2$ random numbers) distributed uniformly within $[-W/2, W/2]$. In principle, each element $\mathcal{W}_{mn}$ could have been chosen as a random number from the interval $[-W, W]$ but the former choice has better similarity with the correlated case. Remarkably, the case with uncorrelated disorder has no analogy with two interacting particle problem but has a simple realization in the optical context. It is worth noting that the pattern structures are rather different for the correlated and uncorrelated cases [compare, e.g., Figs. 5(a) and 5(c)]. In the latter case, the correlations are destroyed. As a consequence, there are no preferable directions visible in the former case, and the pattern acquires an isotropic structure.

Interestingly, statistical properties of level spacing in two- and three-dimensional Anderson models for the noninteracting case have been studied thoroughly in Refs. [19] and [20]. Here, setting different values of disorder, varying the shape of a lattice, and changing the interaction strengths yield additional ways to governing the chaos level of the system, as shown in Fig. 6. For nonzero disorder and U, the probability density function of the spacings s has a tendency to go to the Wigner-Dyson distribution and, as a consequence, a system becomes more chaotic.

In conclusion, in this Rapid Communication we have discussed various interpretations of the optical beam propagation through 2D optical crystals ranging from interacting cold atom dynamics and two-particle Anderson localization to the quantum billiard problems connected with the transition to quantum chaoticity.

The authors are indebted to I. Babushkin, S. Denisov, and N. Li for useful discussions regarding the billiards issues. R.Kh. is supported by RNSF (Grant No. 09/04) and STCU (Grant No. 5053).

[1] P. W. Anderson, Phys. Rev. **109**, 1492 (1958).
[2] T. Schwartz *et al.*, Nature (London) **446**, 52 (2007).
[3] Y. Lahini *et al.*, Phys. Rev. Lett. **100**, 013906 (2008).
[4] J. Billy *et al.*, Nature (London) **453**, 891 (2008); G. Roati *et al.*, *ibid.* **453**, 895 (2008).
[5] M. Gustavsson *et al.*, Phys. Rev. Lett. **100**, 080404 (2008).
[6] O. Morsch, J. H. Muller, M. Cristiani, D. Ciampini, and E. Arimondo, Phys. Rev. Lett. **87**, 140402 (2001); G. Ferrari, N. Poli, F. Sorrentino, and G. M. Tino, *ibid.* **97**, 060402 (2006).
[7] B. P. Anderson and M. A. Kasevich, Science **282**, 1686 (1998); M. Ben Dahan, E. Peik, J. Reichel, Y. Castin, and C. Salomon, Phys. Rev. Lett. **76**, 4508 (1996).
[8] T. Pertsch, P. Dannberg, W. Elflein, A. Brauer, and F. Lederer, Phys. Rev. Lett. **83**, 4752 (1999); R. Sapienza *et al.*, *ibid.* **91**, 263902 (2003); H. Trompeter *et al.*, *ibid.* **96**, 023901 (2006); F. Dreisow *et al.*, *ibid.* **102**, 076802 (2009).
[9] R. Morandotti, U. Peschel, J. S. Aitchison, H. S. Eisenberg, and Y. Silberberg, Phys. Rev. Lett. **83**, 4756 (1999).
[10] A. S. Pikovsky and D. L. Shepelyansky, Phys. Rev. Lett. **100**, 094101 (2008); S. Flach, D. O. Krimer, and Ch. Skokos, *ibid.* **102**, 024101 (2009); M. Johansson, G. Kopidakis, and S. Aubry, Europhys. Lett. **91**, 50001 (2010); T. V. Laptyeva *et al.*, *ibid.* **91**, 30001 (2010); A. Pikovsky and S. Fishman, Phys. Rev. E **83**, 025201(R) (2011).
[11] D. O. Krimer, R. Khomeriki, and S. Flach, Phys. Rev. E **80**, 036201 (2009); A. R. Kolovsky, E. A. Gomez, and H. J. Korsch, Phys. Rev. A **81**, 025603 (2010).
[12] D. M. Jović, Y. S. Kivshar, C. Denz, and M. R. Belic, Phys. Rev. A **83**, 033813 (2011).
[13] A. Perez-Leija *et al.*, Opt. Lett. **35**, 2409 (2010).
[14] S. Longhi, J. Phys. B. (to be published).

[15] H.-J. Stöckmann, *Quantum Chaos: An Introduction* (Cambridge University Press, Cambridge, UK, 1999).

[16] Y. Lahini, Y. Bromberg, D. N. Christodoulides, and Y. Silberberg, Phys. Rev. Lett. **105**, 163905 (2010).

[17] D. O. Krimer, R. Khomeriki, and S. Flach, JETP Lett. **94**, 406 (2011).

[18] M. Karski *et al.*, Science **325**, 174 (2009); A. Peruzzo *et al.*, *ibid.* **329**, 1500 (2010); Y. Lahini *et al.*, e-print arXiv: 1105.2273.

[19] V. E. Kravtsov, I. V. Lerner, B. L. Altshuler, and A. G. Aronov, Phys. Rev. Lett. **72**, 888 (1994).

[20] S. N. Evangelou, Phys. Rev. B **49**, 16805 (1994).